KSME

Springer

Journal of Mechanical Science and Technology 34 (11) 2020

Original Article
DOI 10.1007/s12206-020-1013-7

Keywords:
· Discrete element method
· Multi-body dynamics
· Coupled analysis
· Wheel-soil interaction

Correspondence to:
Jeong-Hyun Sohn
jhsohn@pknu.ac.kr

Citation:
Shin, Y.-J., Jeong, J.-S., Jun, C.-W., Sohn, J.-H. (2020). Interacting analysis between wheel and sand particles based on DEM and its validation with experiments. Journal of Mechanical Science and Technology 34 (11) (2020) 4537~4544.
http://doi.org/10.1007/s12206-020-1013-7

Received May 14th, 2020
Revised August 3rd, 2020
Accepted August 20th, 2020

† Recommended by Editor
No-cheol Park

Interacting analysis between wheel and sand particles based on DEM and its validation with experiments

Yong-Jae Shin[1], Ji-Soo Jeong[2], Chul-Woong Jun[3] and Jeong-Hyun Sohn[4]

[1]Ground Technology Research Institute, Agency for Defense Development, 170 Jayeo-ro, Dong-eup, Changwon-si, Gyeongnam-do 51504, Korea, [2]Department of Naval Architecture & Marine Systems Engineering, Pukyong National Univ., Busan 48513, Korea, [3]VP Corporation, 6-23, Gwangpyeong-ro 51-gil, Gangnam-gu, Seoul, Korea, [4]Department of Mechanical Design Engineering, Pukyong National Univ., Busan 48513, Korea

Abstract It is important to understand the dynamic behavior of a wheel under running condition on the off-road to estimate the tire-soil interaction. The discrete element method is widely used to analyze the dynamic behavior of a wheel driven on a sandy road. A contact method between a wheel and numerous particles was developed to carry out simulation. A wheel testbed experimental setup was established for investigating the contact phenomenon between a wheel and sand particles. A high speed camera was used to capture the motion of the wheel. A clustering model for generating arbitrary shape of a particle was developed. The technique for solving multibody dynamics and particle dynamics simultaneously was suggested. The vertical motion of the wheel by computer simulation was compared with experiments. According to results, the relative error and the root mean square error of the vertical displacement are 5.55 % and 6.05 %, respectively. Simulation results show a good agreement with experiments.

1. Introduction

There are experimental tests and numerical simulations to evaluate the performance of ground vehicles [1]. Due to the complex process and high cost of experimental tests, numerical simulation technology is widely used to evaluate the dynamic performance of vehicles on off-road conditions. It is necessary to validate system dynamics under realistic operating conditions, such as tire-soil interaction when physical testing is not practical. Compared with the experimental test, the evaluation time of numerical simulation is shorter, and it can quickly build a model of track and ground environment. The simulation results can be used to assess the tractive performance under complex road environment and directly provide an important basis for the driving of vehicles. In addition, numerical simulation can reduce test costs and improve calculation efficiency. Therefore, it is required to develop the solver because of this reason. To achieve more reliable and realistic autonomous driving, an algorithm is required to determine the optimum driving speed considering the road and vehicle driving conditions from the viewpoint of vehicle dynamics. Two most important points in this algorithm are real time analysis and safe speed estimation. It is required to calculate the torque necessary to drive the wheels and reduce slip. It is important to understand how to control motors to avoid slip. To solve this problem requires investigating the dynamic behavior of the wheel contacting a soft road such as sandy road and soil. The discrete element method (DEM) is a numerical method used to compute stresses and displacements in volumes containing large numbers of particles, such as grains of sand [2]. The DEM, first proposed by Cundall [3] in 1971, remains the best for simulating particle behavior. This method was originally proposed for rock mechanics applications but has been applied to many granular material problems since 1979 [4, 5].

Recently, DEM has been used to describe the driving road of Mars exploration rover or off-

road vehicles and is used to study contact with wheels [6, 7]. The commercial program, EDEM, is widely used for particle flow simulation by using DEM. Recent, FunctionBay developed an interface module for connecting the RecurDyn and EDEM. Altair motion solver includes the bulk material model from EDEM to combine multibody model and particles. Particle dynamics simulation occurs in repeated stages until the simulation time ends. The first stage involves detecting pairs of colliding particles. Next, the contact force is calculated by using a contact model such as the Kelvin-Voight contact model, comprising spring and damping forces. To carry out vehicle dynamics simulation on a sandy road or soil road, multibody dynamics and particle dynamics should be solved at the same time. Since DEM handles the equations of motion of many particles including contact force, it takes a long time to obtain the results, but it is possible to use a simple integrator. In multibody dynamics with constraints, a higher integrator is needed to solve the constrained equations of motion. Therefore, the proper method is required to connect the DEM solver and multibody dynamics solver. In addition, the endeavor to reduce the computational time is needed to perform a computer simulation with many particles. The parallel computing has been used to reduce the calculation time. Especially, many studies using the graphic processing unit (GPU) based parallel computing have been carried out and shown good results. NVIDIA introduced the compute unified device architecture (CUDA) platform for GPU based parallel computing in 2007 [8].

This paper proposes to identify the interacting action between a wheel and sand particles. When a wheel runs on a sandy road, the road experiences deformation due to contact with a wheel. The road shape and the dynamic behavior of the wheel are considered. In this study, an interacting analysis between the wheel and sand particles was carried out. For the coupled analysis, the coupled program, Xdynamics, was developed. Xdynamics solved the coupled problem between multibody dynamics and particle dynamics based on GPU parallel computing. The wheel testbed experimental device was established for validating the computer simulation. A high speed camera was used to capture the motion of the wheel. The vertical motion of the wheel was compared with experiments.

2. Discrete element method

2.1 Equations of motion of particles

In DEM formulation, each particle has a mass, an inertia and a radius. Contact forces from neighboring particles cause each particle to move. Eqs. (1) and (2) are the equations of motion for each particle.

$$m_i \dot{v}_i = \left(\frac{4}{3} r_i \pi r_i^2\right) \dot{v}_i = f_i \tag{1}$$

$$I_i \dot{\omega}_i = \left(\frac{2}{5} m_i r_i^2\right) \dot{\omega}_i = T_i \tag{2}$$

where $r_i, m_i, \boldsymbol{v}_i, I_i, \boldsymbol{f}_i, \boldsymbol{T}_i, \boldsymbol{\omega}_i$ are the radius, mass, velocity, inertia, external force, torque and angular velocity of the i[th] particle, respectively. The particle's position, velocity, and angular velocity at a given time can be calculated by using the velocity-Verlet integration algorithm given by Eqs. (3)-(5).

$$\boldsymbol{r}_i(t+\Delta t) = \boldsymbol{r}_i(t) + \boldsymbol{v}_i(t)\Delta t + \frac{\boldsymbol{f}_i(t)\Delta t^2}{2m_i} \tag{3}$$

$$\boldsymbol{v}_i(t+\Delta t) = \boldsymbol{v}_i(t) + \frac{\left(\boldsymbol{f}_i(t) + \boldsymbol{f}_i(t+\Delta t)\right)\Delta t}{2m_i} \tag{4}$$

$$\boldsymbol{\omega}_i(t+\Delta t) = \boldsymbol{\omega}_i(t) + \frac{\left(\boldsymbol{T}_i(t) + \boldsymbol{T}_i(t+\Delta t)\right)\Delta \mathrm{t}}{2I_i} \tag{5}$$

where Δt is the time interval and t means the time. $\boldsymbol{r_i}$, I_i are the position and moment of inertia of i[th] particle, respectively. Unlike explicit Euler method, the velocity-Verlet algorithm assumes that acceleration depends on the position rather than velocity. Therefore, the velocity and angular velocity are calculated after the forces are calculated because the velocity and angular velocity are calculated by the force and moment at the time t and $t+\Delta t$. Contact detection and force calculation are calculated by using the updated position.

2.2 Contact detection and forces

In this study, the two-phase contact detection approach which includes a broad phase followed by a narrow phase was used. In a broad phase, collision tests are based only on bounding volumes and are conducted quickly to immediately eliminate non-colliding object pairs. Output from the broad phase is a set of potentially colliding objects pairs. In the narrow phase, collision tests are performed only for this set of potentially colliding object pairs. This approach is proper when numerous objects are considered. In this study, spatial subdivision resulted in many non-colliding object pairs, which were rejected during the broad phase. Contact detection is classified into three cases: particle-particle, particle-boundary, and particle-object. In this study, the neighboring cell technique was used for contact detection [3].

Contact force is basically calculated by using the penetration between particle-particle or particle-object. The contact force is composed of the normal force and tangential force. In this study, the damped Hertzian spring model, proposed by Taguchi and Ristow, was used to determine contact force [9-11]. Fig. 1 shows the contact force model. The normal force is calculated by using the spring constant, damping coefficient, and penetration. The tangential contact force due to sliding friction, the tangential spring constant, tangential damping coefficient, and tangential displacement determined the tangential contact force. The lower value of two becomes the final tangential contact force.

The summation of the spring force and damping force becomes the normal contact force like Eq. (6).

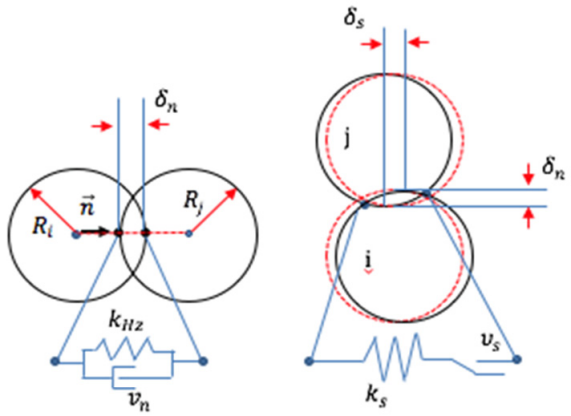

Fig. 1. Contact force model.

$$\boldsymbol{F}_n = \left(-k_n\delta_n^{3/2} + v_n\Delta\boldsymbol{v}_n \cdot \boldsymbol{n}\right)\cdot \boldsymbol{n} \tag{6}$$

$$\Delta\boldsymbol{v}_n = \boldsymbol{v}_j + \boldsymbol{\omega}_j \times R_j\left(-\boldsymbol{n}\right) - \boldsymbol{v}_i + \boldsymbol{\omega}_i \times \boldsymbol{R}_i\,\boldsymbol{n} \tag{7}$$

where k_n is the Hertzian stiffness and v_n is the normal damping constant. $\Delta\boldsymbol{v}_n$ as shown in Eq. (7) is the relative velocity between two particles. δ_n means the overlap between the particle I and particle j and **n** is the normal unit vector. The tangential contact force is determined by using Eq. (8) as follows:

$$\boldsymbol{F}_t = \min\left\{k_s\delta_s + v_s\Delta\boldsymbol{v}_s \cdot \boldsymbol{s}; \mu_s\left|\boldsymbol{F}_n\right|\right\}\cdot \mathbf{s} \tag{8}$$

$$\Delta\boldsymbol{v}_s = \Delta\boldsymbol{v}_n - \left(\Delta\boldsymbol{v}_c \cdot \boldsymbol{n}\right)\cdot \boldsymbol{n} \tag{9}$$

where k_s is the tangential spring constant, $\boldsymbol{v}_s$ is the tangential damping coefficient, and u_s is the tangential sliding friction coefficient. The friction coefficient is a measure of the amount of friction existing between two surfaces. The lower friction coefficient indicates that it is possible to generate the sliding motion with weak friction force. $\Delta\boldsymbol{v}_s$ as shown in Eq. (9) is the relative tangential velocity between. The tangential unit vector is given as $\mathrm{s} = \Delta\boldsymbol{v}_s / \left|\Delta\boldsymbol{v}_s\right|$ and the tangential displacement is added to the accumulated rolling deformation vector from the last time step as $\delta_s^n = \delta_s^{n-1} + \left|\Delta\boldsymbol{v}_s^n\right| \times \Delta t$. The moment resulting from the tangential contact force is calculated by using Eq. (10)

$$\boldsymbol{M}_i = \left(R_i \cdot \boldsymbol{n}\right) \times \boldsymbol{F}_t\,. \tag{10}$$

Eq. (11) is used to calculate the relative velocity between the particle and the boundary for the contact force.

$$\Delta\boldsymbol{v} = -\left(\boldsymbol{v}_i + \boldsymbol{\omega} \times R_i\boldsymbol{n}\right). \tag{11}$$

Hertzian stiffness is calculated by using Young's modulus and Poisson's ratio in Eq. (12) as follows:

$$k_n = \frac{4}{3}\sqrt{R^*}E^{\cdot} \tag{12}$$

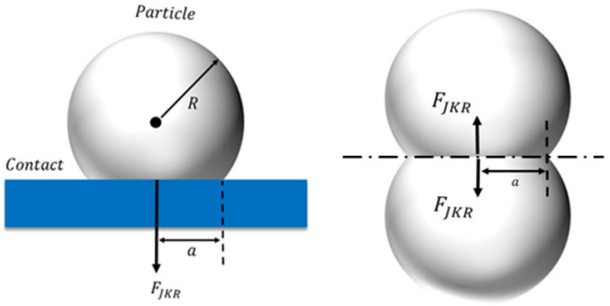

Fig. 2. Adhesive force model.

$$\frac{1}{R^*} = \frac{1}{R_i} + \frac{1}{R_j} \tag{13}$$

$$\frac{1}{E^*} = \frac{1-\nu_i^2}{E_i} + \frac{1-\nu_j^2}{E_j} \tag{14}$$

where $E_{i,j}, \nu_{i,j}, R_{i,j}$ are Young's modulus, Poisson's ratio, and radii of the i[th] and j[th] particles, respectively. R^*, E^* are the effective radius and Young's modulus.

The adhesive force developed by Johnson-Kundall-Robert in 1971 was used in this study [12, 13]. In this model, the surface energy between particles is considered. Fig. 2 shows the schematic of the cohesive model.

Eq. (15) represents the adhesive force:

$$\boldsymbol{F}_{JKR} = -2\sqrt{2\pi\gamma E^* a^3}\cdot \boldsymbol{n} \tag{15}$$

$$a^3 = \frac{3R^*}{4E^*}\left(F_n + C_\gamma + \sqrt{2C_\gamma F_n + C_\gamma^2}\right) \tag{16}$$

$$C_\gamma = 3\gamma\pi R^* \tag{17}$$

where γ is adhesive energy, a^3 is JKR contact radius. The adhesive energy is the energy released when one particle comes in contact with another particle surface. The adhesive force is considered as the normal force in contact between particles, such as spring force and damping force.

2.3 Cluster particle modeling

Generally, sand particles have several shapes, such as rectangular, cylindrical and spherical. To consider these types of particles, the cluster particle was established in this study [14]. The main advantage of the use of spheres is their lower computational cost, but there is a limit to the geometrical contact motion of real sand. Clusters of spheres are developed for describing the movement of each particles, specifically, the imposition of the rolling friction and the integration of the rotation of clusters of spheres. Fig. 3 represents the cluster model of sand particles used in this study. Fig. 4 shows the coordinate system of cluster particle model which consisted of four particles. The clusters of spheres approach consists of representing each particle as a group of overlapping spheres joined rigidly, thereby allowing the use of algorithms that are straightforward

Table 1. Modeling parameter of sphere and cluster model.

Item	Sphere	Cluster
Particle radius (mm)	2.5	
No of particles	1	4
Friction coefficient	0.4 / 0.4	
Total particles	31329	49392
Size of cube (mm^3)	300*400*300	300*300*300
Initial height (mm)	50	
Wheel mass (kg)	3.31	

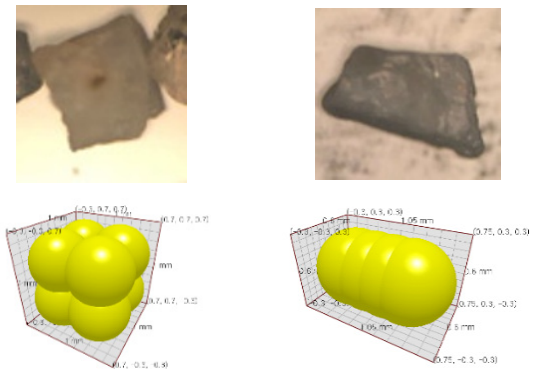

Fig. 3. Cluster model of sand particles.

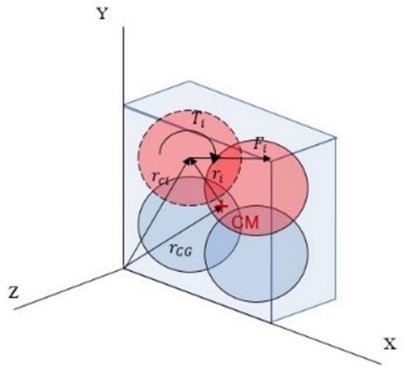

Fig. 4. Coordinate system of cluster particle model.

extensions of the efficient methods used for spheres.

In this study, the cluster model was compared with sphere model for two cases. First, the porosity of sphere model and cluster model was compared. As shown in Table 2, the volume of cluster model is the same as the sphere model. Then the height of each model is changed due to the self-weight. The height of the cluster model is lower than sphere model as shown in Table 2. Therefore, cluster model is dense and can support the wheel well. Next, the wheel contact was tested in cases of cluster model and sphere model. Table 3 represents the comparison of wheel contact for cluster model and sphere model. Fig. 5 shows the vertical displacement of the wheel for both models. According to the results, the cluster model supports the wheel more than the sphere model. Therefore, the cluster model was used for wheel testbed simulation in this study.

Table 2. Comparison of porosity for cluster model and sphere model.

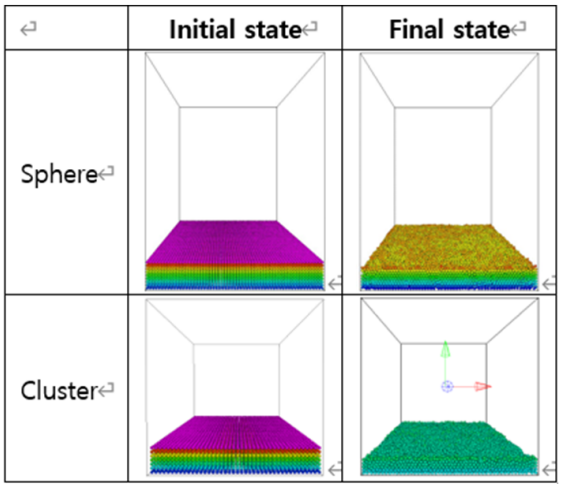

Table 3. Comparison of wheel contact for cluster model and sphere model.

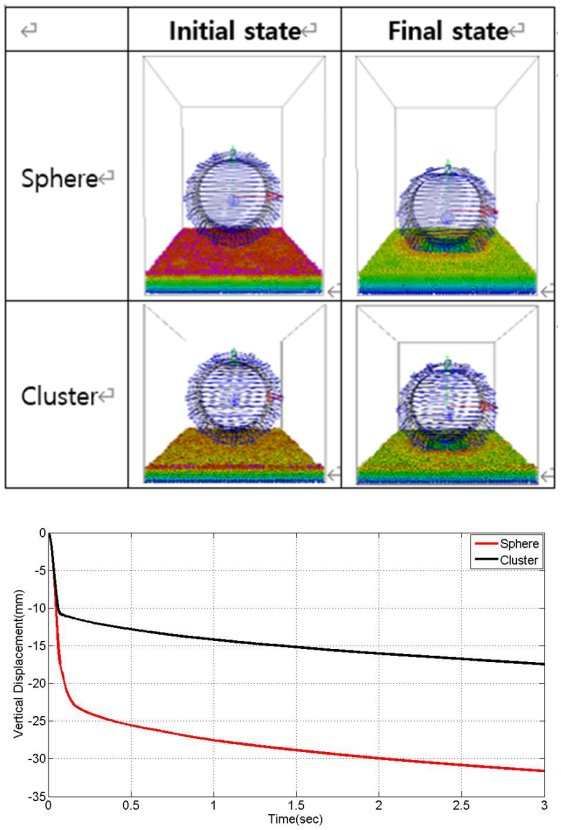

Fig. 5. Vertical displacement of both models.

The procedure of the contact force calculation in the cluster model is represented in Fig. 6. In the first stage, the contact between particles is detected and the amount of penetration of contact is calculated. Next, the contact force is calculated and it is transferred to forces and torques at the center of mass. The force and moment contribution obtained from each particle is

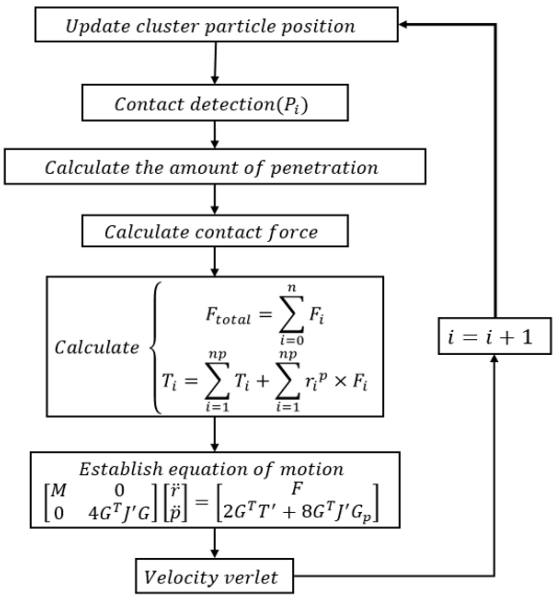

Fig. 6. Solving procedure of cluster model.

then summed up and transferred to the center of mass the cluster. Finally, the equations of motions are established and are solved by using velocity-Verlet algorithm. In Fig. 6, $\boldsymbol{r}_i^p$ is a vector from the center of cluster to each particle i.

3. Wheel testbed experiment

Fig. 7 shows the wheel appearance and dimensions used in this study. The number of teeth is 16 and the width of teeth is 100 mm. The outer diameter and inner diameter of the wheel are 200 and 180 mm, respectively. The rover wheel shape was considered for clarifying the interacting motion between the wheel and sandy roads. Fig. 8 shows the tracking marker position for measuring the wheel motion. The testbed can move in the longitudinal direction and vertical direction by using the motor control. The wheel with 100 mm radius can rotate by using the rotary motor. Fig. 9 represents the experimental setup for the wheel test. As shown in Fig. 8, a tracking marker is attached at the moving body and the sinkage can be measured by using a high-speed camera. The wheel moves with 10 mm/s in the longitudinal direction and rotates with 0.1 rad/s. In this study, a high-speed camera with 3000 fps was used for capturing the dynamic behavior of the wheel. The test procedure is as follows:

a) The wheel and sensors are lifted up.

b) The sandy road is set to be smoothing.

c) The wheel and sensors are placed on the sandy road slowly. Just after contacting with a wheel, the sandy road experiences deflection. This operating work is done manually, not automatically. Therefore, it is possible to be different condition at each time.

d) The wheel is rotated with constant velocity.

e) A high speed camera is used to capture the dynamic motion of the wheel.

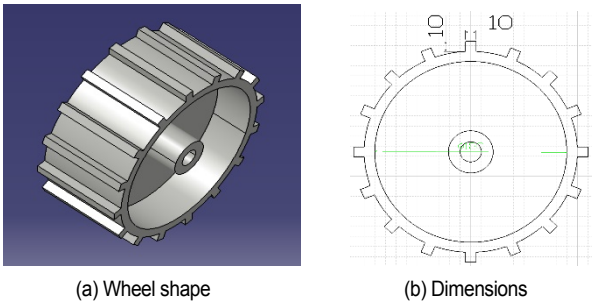

(a) Wheel shape (b) Dimensions

Fig. 7. Wheel shape and dimensions.

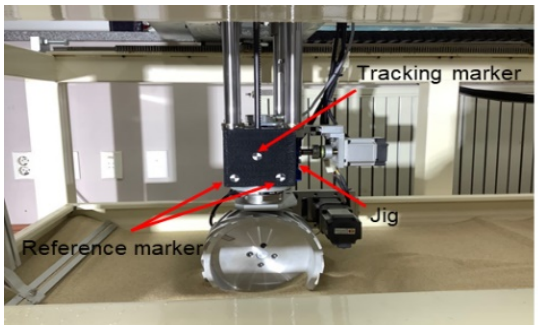

Fig. 8. Tracking marker position for measuring the wheel motion.

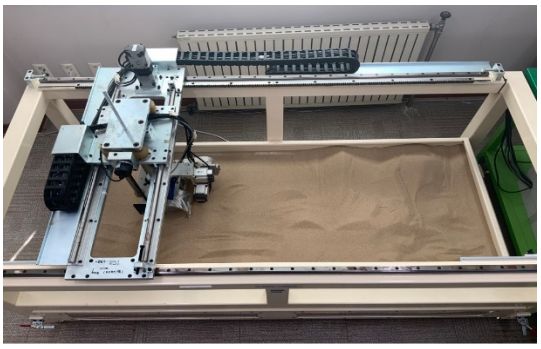

Fig. 9. Experimental setup for wheel test.

f) After 10 s, the wheel stops.

g) After the test, the wheel and sensors are lifted up and moved to the initial position.

4. Interacting analysis between wheel and sand particles

A coupled analysis program of DEM and MBD, Xdynamics was developed. The main solver was developed by using the C++ language with Visual Studio 2017. GPGPU based parallel computing [8] was used for the numerical calculation. Qt open source was used for GUI(graphic user interface) programming, and OpenGL was employed to display graphically the analysis model and result. Fig. 10 shows the block diagram of main processor. There are several objects such as particles, rigid bodies, constraints, contacts and forces. The revolute joint, spherical joint, translational joint and universal joint are in-

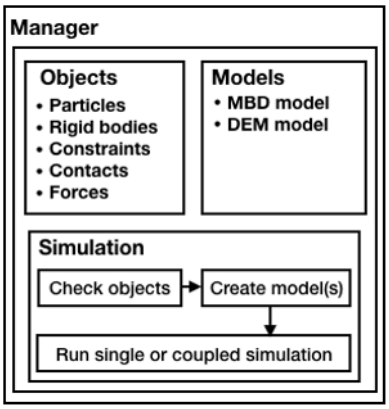

Fig. 10. Block diagram of main processor.

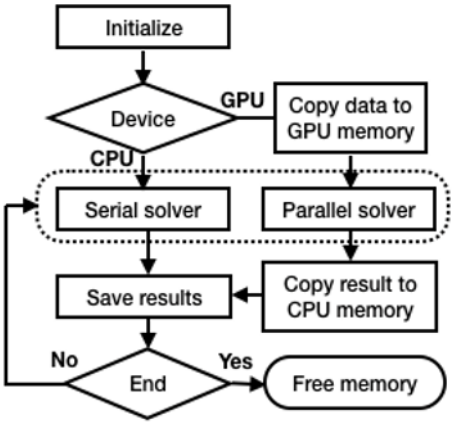

Fig. 11. Block diagram of the simulation process.

cluded for generating the constraints of multibody dynamics. Force element includes the translational spring damper actuator, the rotational spring damper actuator and contact model between particle-particle and particle-rigid body. Fig. 11 represents the block diagram of the simulation process. At the beginning stage, all the parameters are initialized. Next, data is copied to GPU memory and simulation is carried out by using parallel solver at GPU and results are copied to CPU memory and all data are saved. Fig. 12 shows the flow chart for coupled analysis. In the first stage, all the parameters are initialized. Next, the contact between the rigid body and particles is detected and the contact force is calculated. The contact force is applied to the rigid body and particles, respectively. Then, MBD solver and DEM solver are running and data is updated.

Road shape has 700 mm*260 mm*50 mm and is shown in Fig. 13. Two sizes of cluster models were used in this study. To represent the real sandy road, two sizes of cluster were needed to be mixed equally. Mixing procedures are as follows: (a) Lower part of sandy road has small size of cluster and big size of cluster is placed on the upper part. (b) An instant rotational motion is applied to the road boundary and then the cluster moves rapidly due to impact motion. (c) After several seconds, clusters are placed and mixed with each other.

The outline of the wheel has 530000 triangular elements for

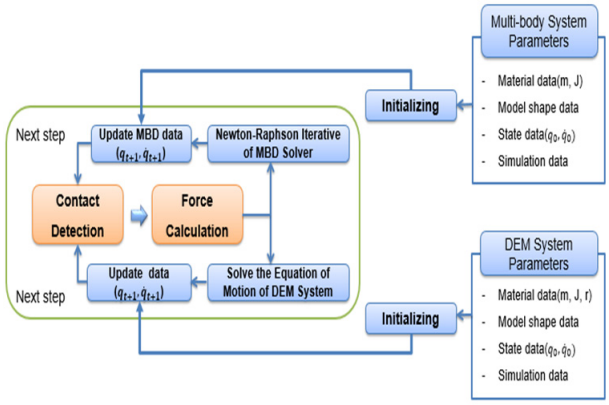

Fig. 12. Flow chart for coupled analysis.

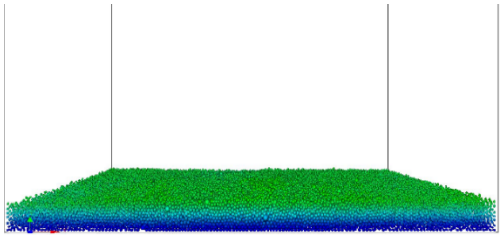

Fig. 13. Road generation.

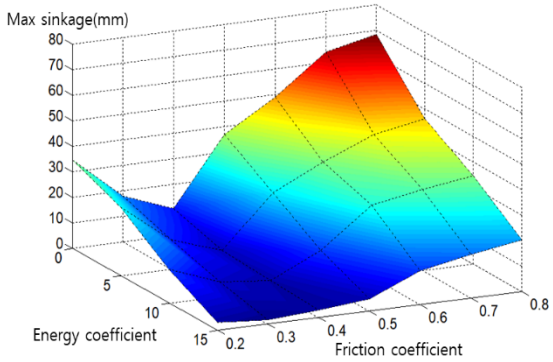

Fig. 14. Sinkage according to friction coefficient and energy coefficient.

contact simulation with particles. It is very difficult to find the proper contact parameters between the wheel and sandy particles. Therefore, in this study, six types of friction coefficients (0.2, 0.3, 0.4, 0.5, 0.6, 0.7) and four types of energy coefficients (0, 5, 10, 15) were chosen for determining the proper parameters. Fig. 14 represents the sinkage according to the friction coefficient and adhesive coefficient. According to the parameter study, it is noted that 0.4 of friction coefficient and 15 adhesive coefficient gives more accurate results. Table 4 shows the parameters used in the simulation. Young's modulus and sand density were chosen as the representative value of the sand. Table 5 represents the computer specifications used in this study. Fig. 15 shows the simulation pictures at each time step. When the wheel runs on the sandy road, the sandy particles are pushed back and piled up at some height. The wheel makes a sinkage on the sandy road as shown in the experi-

Table 4. Parameters used in simulation.

Type	Values
Sand Young's modulus	400000 GPa
Friction coefficient, adhesive coefficient	0.4, 15
Diameter of particles	5.0 mm, 2.5 mm
Number of clusters	13608, 140000
Size of boundary areas	903 mm*260 mm*50 mm
Sand density	2406 kg/m^3

Table 5. Computer specifications.

Item	Spec	Details
CPU	i9-9900K	Clocks: 4.6 GHz Core: 8 Threads: 16 Reversion: P0
GPU	NVIDIA TITAN RTX	Size: 24 GB Type: GDDR6 Reversion: A1
RAM	64 GB	Type: DDR4 Channel#: Dual

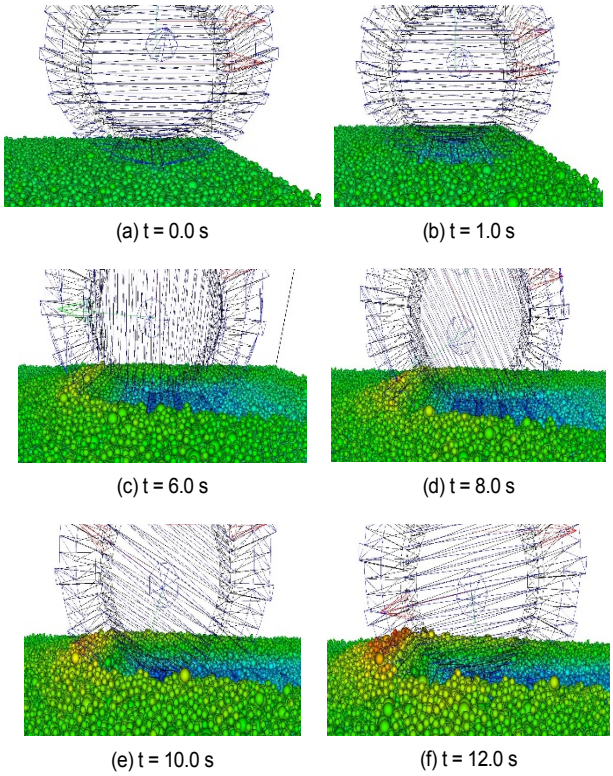

(a) t = 0.0 s (b) t = 1.0 s (c) t = 6.0 s (d) t = 8.0 s (e) t = 10.0 s (f) t = 12.0 s

Fig. 15. Simulation pictures.

ments. The computational time for 12 s simulation was about 120 hours.

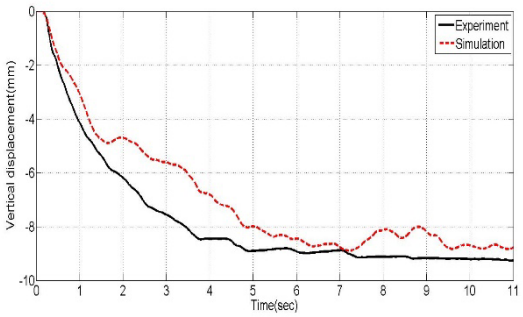

Fig. 16. Comparison of vertical displacement.

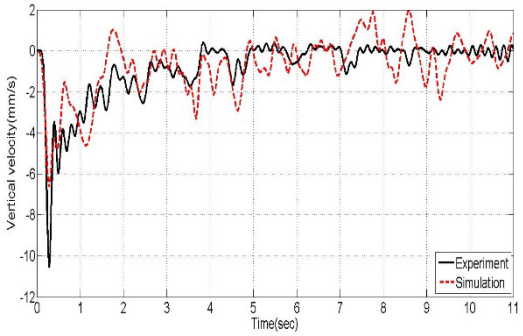

Fig. 17. Comparison of vertical velocity.

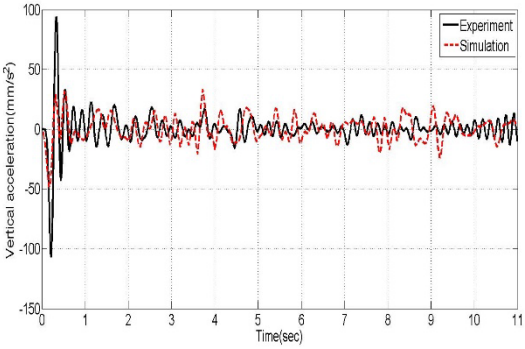

Fig. 18. Comparison of vertical acceleration.

5. Comparison of simulation results with experiments

Figs. 16-18 represent the comparisons of displacement, velocity and acceleration of simulation and experiments. Simulation results show good agreement with experiments in terms of the tendency. When the wheel runs on the sandy road, the difference of vertical displacement between the simulation and experiment is less than 10 %. After 7 sec, the vertical displacement approaches the stable position. The error for data after 7 sec is calculated. The relative error and RMS error for the vertical displacement are 5.55 % and 6.05 %, respectively. It is impossible to exactly generate the road condition and shape of millions of particles having several shapes. Therefore, this method can be available to estimate the tire-sandy road interactions.

6. Conclusions

An interactive analysis between a wheel and sand particles was carried out. For the wheel test bed simulation, Xdynamics which is house-code, was used. The wheel testbed experimental device was established for validatingthe computer simulation. The vertical motion of the wheel was compared with experiments.

1) A coupled analysis program between multibody dynamics and discrete element method was developed in this study.

2) To validate the dynamic behavior of the wheel under the sandy road condition, an experimental device was established and experiments were performed. When the wheel ran on a sandy road, the difference of vertical displacement between the simulation and experiment was less than 6 %. It is very difficult to represent the road condition and shape of millions of sandy particles having several shape exactly. Therefore, this method can be a candidate to estimate the tire-sandy road interaction. This method can be useful to the contact analysis between the wheel and sandy particles.

Acknowledgments

This research was supported by Basic Science Research Program through the National Research Foundation of Korea (NRF) funded by the Ministry of Education (2018R1D1A1 07050817).

References

[1] Y. S. Pyoun, Y. D. Jang, J. H. Park and I. H. Cho, Y. C. Lee, A study on development of test methodology and test of no spin differential for off-road vehicle, *Transactions of KSAE*, 13 (4) (2005) 32-38.

[2] J. H. Lee and W. S. Yoo, Study on the 3D virtual ground modeling and application for real-time vehicle driving simulation on off-road, *Transactions of KSAE*, 18 (4) (2010) 92-98.

[3] P. A. Cundall and O. D. L. Strack, A discrete numerical model for granular assemblies, *Geotechnique*, 29 (1979) 47-65.

[4] A. Datta, B. K. Mishra, S. P. Das and A. Sahu, A DEM analysis of flow characteristics of noncohesive particles in hopper, *Materials and Manufacturing Processes*, 23 (2) (2008) 195-202.

[5] W. Smith, D. Melanz, C. Senatore, K. Iagnemma and H. Peng, Comparison of discrete element method and traditional modeling methods for steady-state wheel-terrain interaction of small vehicles, *Journal of Terramechanics*, 56 (2014) 61-75.

[6] J. B. Johnson, A. V. Kulchitsky, P. Duvoy, K. Iagnermma, C. Senatore, R. E. Arvidson and J. Moore, Discrete element method simulations of Mars Exploration Rover wheel performance, *Journal of Terramechanics*, 62 (2015) 31-40.

[7] J. Mingjing, D. Yongsheng, C. Liang and X. Banglu, Experimental and DEM analyses on wheel-soil interaction, *Journal of Terramechanics*, 76 (2018) 15-28.

[8] NVIDIA, *CUDA C Programming Guide v7.5*, NVIDA Corporation (2015).

[9] C. Ericson, *Real-time Collision Detection*, Morgan Kaufmann Publishers, San Francisco (2005) 50-52.

[10] A. Recuero, R. Serban, B. Peterson, H. Sugiyama, P. Jayakumar and D. Negrut, A hogh-fidelity approach for vehicle mobility simulation: Nonlinear finite element tires operating on granular material, *Journal of Terramechanics*, 72 (2017) 39-54.

[11] C. W. Jun, Study on contact analysis between spatial multibody system and many particles using GPGPU, *Master Dissertation*, Pukyong National University, Busan (2013).

[12] K. L. Johnson, K. Kendall and A. D. Roberts, Surface energy and the contact of elastic solids, *Proc. Roy. Soc. London A* (1971) 324:301-313.

[13] E. Barthel, Adhesive elastic contacts – JKR and more, *Journal of Physics D: Applied Physics*, 41 (16) (2008) 163001.

[14] J. Isazábal González, Numerical analysis of railway ballast behavior using the discrete element method, *Ph.D. Thesis*, Monograph CIMNE (2017).

Yong Jae Shin is a researcher for Ground Technology Research Institute at ADD, Korea. His research interests include multibody system dynamics and terramechanics.

Ji Su Jeong is an undergraduate student in Mechanical Design Engineering at Pukyong National University, Busan, Korea. His research interests include multibody dynamics and robot control.

Chul Woong Jun is a researcher for VP Korea Inc., Seoul, Korea. His re-search interests include vehicle dynamics and dynamic analysis of multibody system.

Jeong Hyun Sohn is Professor of the Department of Mechanical Design Engineering at Pukyong National University, Busan, Korea. His research interests include mechanism design and multibody system dynamics.